Int. J. Heat Mass Transfer. Vol. 36, No. 12, pp. 3107–3117, 1993
Printed in Great Britain

0017–9310/93 $6.00+0.00

Comparison of natural convection of water and air in a partitioned rectangular enclosure

JAMIL A. KHAN and GUANG-FA YAO
Department of Mechanical Engineering, University of South Carolina, Columbia, SC 29208, U.S.A.

(*Received* 7 *August* 1992 *and in final form* 25 *November* 1992)

Abstract—A numerical solution comparing steady natural convection of water and air in a two dimensional, partially divided, rectangular enclosure is presented. Rayleigh numbers investigated range from 10^6 to 10^8, and the opening ratios studied are 0, 1/4, 1/6, and 1/8 respectively. To obtain a comparative study, Prandtl number of 7.0 (for water) and Prandtl number of 0.71 (for air) are used for the two working fluids. This study demonstrates that the conventional use of water to model air convection in partitioned enclosures gives reasonable heat transfer results. The average Nusselt number obtained for water is only 2 ~ 5% larger than that for air at the same conditions. The flow configuration and exchange flow rates for water and air are, however, different. The exchange flow rate for water is found to be 10 ~ 20% larger than that for air. It is observed that for the opened partition the average Nusselt number is 13 ~ 24% larger than that for unopened partition. On the other hand, an opening in the partition reduces the exchange volume flow rates by 5.68 ~ 15.2% for water and 1 ~ 11.4% for air, depending on the Rayleigh number and the opening ratio.

INTRODUCTION

NATURAL convection heat transfer and fluid flow in partitioned enclosures has received considerable attention during the past decade because of its practical application in solar collector design, indoor air quality investigation, fire spread and energy conservation in rooms and buildings, and cooling of nuclear reactors, etc. In the study of ventilation and indoor air quality the measure of exchange volume flow rates between rooms is very important, because the exchange flow rates is a measure of contaminant exchange between the rooms.

Brown and Solvason [1] conducted experimental investigation of natural convection heat and mass transfer through a small opening in a vertical partition between two chambers. Brown [2] in the second part of his study investigated flow between two chambers with a horizontal partition. This experimental investigation is one of the very few experimental studies where air was used as the experimental fluid. In most of the other experimental works, water, brine or kerosene were used to model air flow between chambers. Epstein [3] and Epstein and Kenton [4] made experimental investigations of buoyancy-driven exchange flow between two chambers. Their experiments were performed using brine and fresh water to simulate the effect of a density difference. Since brine solution was used to model air transport, viscous and temperature effects were neglected in their work. The neglect of this effect was discussed and justified by comparison with the air data of Brown [2]. Bejan and Rossie [5] studied natural convection flow between two reservoirs connected by a horizontal two dimensional duct with length and width approximately equal to those of the chambers. Lin and Bejan [6] also carried out an experimental study of natural convection in a partially divided enclosure, using water as the working fluid. Neymark *et al.* [7] investigated the phenomenon of natural convection of air and water in a partially divided enclosure, aiming to determine the effect of an internal partition on the natural convection heat transfer across the enclosure. Nansteel and Greif [8] made an investigation of natural convection in enclosures with two and three dimensional partition. In another work Nansteel and Greif [9] investigated the effect of two dimensional conducting and nonconducting centrally located partition of various lengths extending vertically downwards from the ceiling of a water-filled rectangular enclosure. Chen *et al.* [10, 11] performed experimental and numerical research which is similar to the two dimensional partition case in ref. [8] with and without opening in partition. In their work they used water as the working fluid. For the experimental work [10] they used isothermal boundary conditions for the two vertical walls, whereas, for the numerical work [11] they used constant heat flux boundary conditions for the vertical walls. They also studied the effect of conductivity of the partition wall and concluded that the conductivity of the partition wall did not have any significant effect on the heat transfer rates. Chang *et al.* [12], Acharya *et al.* [13, 14] and Shaw *et al.* [15] made a series of numerical investigations of natural convection in a square cavity with vertical partial divisions extending upwards from the enclosure floor and downwards from the ceiling simultaneously. The effects of partition height, thickness and transverse position were examined in their

NOMENCLATURE

A	aspect ratio, L/H
A_o	opening ratio, s/h
A_p	partition ratio, h/H
g	acceleration due to gravity
H	enclosure height
h	height of partition plate
k	thermal conductivity of the fluid
L	enclosure length
Nu	average Nusselt number
Pr	Prandtl number, ν/α
Q	volumetric exchange flow rate at the partition plane
Ra	Rayleigh number, $g\beta H^3(T_h-T_l)/(\alpha\nu)$
s	opening size
T	temperature
T_h	temperature of hot wall
T_l	temperature of cold wall
u	horizontal velocity component
U	nondimensional horizontal velocity component, uH/ν
v	vertical velocity component
V	nondimensional vertical velocity, vH/ν
x	horizontal coordinate
X	nondimensional horizontal coordinate, x/H
y	vertical coordinate
Y	nondimensional vertical coordinate, y/H.

Greek symbols

α	thermal diffusivity of the fluid
β	thermal expansion coefficient of the fluid
θ	dimensionless temperature, $(T-T_l)/(T_h-T_l)$
ν	kinematic viscosity, μ/ρ
ρ	fluid density
ρ_0	fluid density at reference temperature.

work. In Acharya's work, the effect of a conducting and nonconducting partition was also studied. Fu *et al.* [16] dealt with transient laminar natural convection in an enclosure partitioned by an adiabatic baffle using a finite element method and explored the effect of the baffle position and Rayleigh number on the fluid flow and heat transfer mechanism. All of these numerical investigations were for Rayleigh numbers of 10^6 or less.

The works mentioned above have the following characteristics: (1) Experimental work uses water as the working fluid to model air flow. This is done for the sake of experimental convenience. Rayleigh numbers investigated experimentally are very high (as high as 10^{11}). (2) Numerical works use air as the working fluid and Rayleigh numbers investigated in most cases are less than 10^6. This is done because at higher Rayleigh numbers the numerical solution lends itself to numerical instability, well before the actual flow becomes turbulent (Lee and Dulikravich [17]).

However, in most cases of practical interest, the working fluid is air and Rayleigh number is larger than 10^6. Therefore, to predict meaningful practical results there is a need to investigate natural convection flow in enclosures at higher Rayleigh numbers. The objectives of the present study are: to obtain a numerical solution of natural convection at higher Rayleigh numbers; and to compare the heat and mass transfer results for both air and water. The comparison of the heat transfer and volume exchange flow rates for water and air are carried out to investigate the applicability and efficiency of using water models to predict the natural convection results for air. The physical domain chosen for the current investigation is the same as in refs. [10, 11], with an aspect ratio of $A = L/H = 2$, a partition ratio $A_p = h/H = 1/2$, and opening ratios of $A_o = s/h = 0$, 1/4, 1/6, 1/8.

PHYSICAL MODEL

The geometry and boundary conditions for the problems investigated in this study are shown in Fig. 1. The two horizontal walls are considered insulated while the two vertical walls are maintained at two different temperatures T_h and T_l respectively. The partition is assumed to be insulated. The parametric study includes investigations for partitions with and without opening ($A_o = 0$, 1/4, 1/6, 1/8).

In the present model the flow is simulated as a two dimensional phenomenon with the following assumptions/simplifications:

(1) The fluid is Newtonian, incompressible and the flow is laminar.
(2) Boussinesq approximation is invoked and
(3) Radiation effects are neglected.

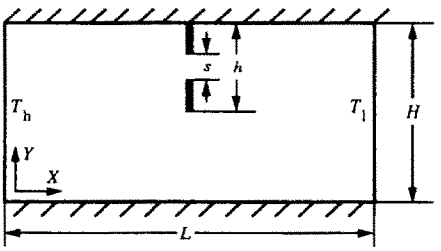

FIG. 1. Geometry and boundary conditions.

With the above assumptions and the introduction of the following dimensionless variables;

$$X = \frac{x}{H}, \qquad Y = \frac{y}{H},$$

$$U = \frac{uH}{\nu}, \qquad V = \frac{vH}{\nu}$$

$$\theta = \frac{T - T_1}{T_h - T_1}, \qquad P = \frac{(p + \rho_o gy)(H^2)}{\rho_o \nu^2}$$

$$Pr = \frac{\nu}{\alpha}, \qquad Ra = \frac{g\beta H^3 (T_h - T_1)}{\alpha\nu}. \tag{1}$$

The governing differential equations that express the conservation of mass, momentum and energy in the fluid domain become:

$$\frac{\partial U}{\partial X} + \frac{\partial V}{\partial Y} = 0 \tag{2}$$

$$U\frac{\partial U}{\partial X} + V\frac{\partial U}{\partial Y} = -\frac{\partial P}{\partial X} + \left(\frac{\partial^2 U}{\partial X^2} + \frac{\partial^2 U}{\partial Y^2}\right) \tag{3}$$

$$U\frac{\partial V}{\partial X} + V\frac{\partial V}{\partial Y} = -\frac{\partial P}{\partial Y} + \left(\frac{\partial^2 V}{\partial X^2} + \frac{\partial^2 V}{\partial Y^2}\right) + \frac{Ra\theta}{Pr} \tag{4}$$

$$U\frac{\partial \theta}{\partial X} + V\frac{\partial \theta}{\partial Y} = \frac{1}{Pr}\left(\frac{\partial^2 \theta}{\partial X^2} + \frac{\partial^2 \theta}{\partial Y^2}\right) \tag{5}$$

the non-dimensional Nusselt number, Nu, and volumetric exchange flow rate, Q, are defined as below:

$$Nu = \int_0^1 \left[U\theta - \frac{\partial \theta}{\partial X}\right] dY$$

$$Q = \frac{1}{2}\int_0^1 |U|\, dY \tag{6}$$

where, H is the height of the duct, θ, X and Y are nondimensional temperature and spatial coordinates respectively.

NUMERICAL PROCEDURE

Equations (2)–(5) are discretized utilizing a method called practice B [18] which is a control volume based finite difference method. To avoid checker-board pressure and velocity fields, a staggered grid is used for the velocity in the X and Y directions. The power law profile approximations recommended by ref. [18] are made in each coordinate direction. The resulting algebraic equations are solved iteratively using a line by line Thomas Algorithm. A rectangular calculation domain was adopted for convenience. The presence of solid area is accounted for by a strategy developed by Patankar [19] in which the governing equations along with the boundary conditions are solved for the complete domain with the solid area characterized by a very high (10^{30}) viscosity and zero conductivity. The high viscosity and zero conductivity satisfies the requirement of adiabatic wall with no-slip velocity boundary condition.

A SIMPLE-like algorithm developed by Date [20] is used to treat the coupling of momentum and energy equations. In this method, at every iteration level, the solution of discretization equations consist of two stages, prediction stage and correction stage. At prediction stage, the SIMPLE algorithm is invoked to obtain pressure and velocity correction values which are used as prediction values. Using prediction values of pressure and velocity and incorporating the effects of convection, diffusion and source term, a pressure correction equation is solved again to obtain correction values of pressure and velocity. Finally the values of pressure and velocity are obtained at the iteration level. The coefficients of this pressure correction are the same as those in the SIMPLE algorithm except for the source terms which include the effects of convection and diffusion and source terms here. In the present work, effects of adjacent nodes are neglected, only the changes of source terms between two successive iterations are considered. The relaxation factor for velocity is 0.5. The relaxation factor for calculating pressure is only used in some cases. Calculations performed using this method resulted in good convergence rates, especially at higher Rayleigh numbers.

The convergence criterion was varied and grid

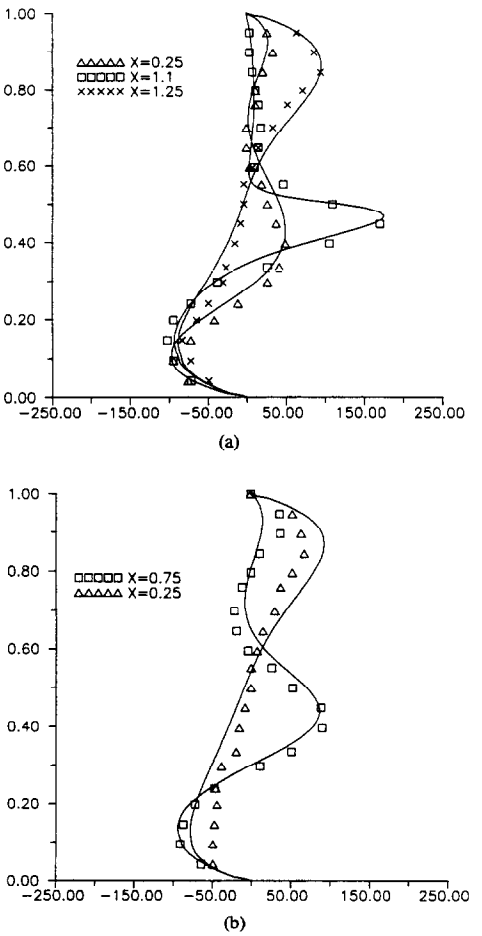

FIG. 2. Comparison of numerical and experimental results; velocity profiles at $X = 0.25, 0.75, 1.1, 1.25, 1.75$, $Ra = 10^6$.

Table 1. Comparison of numerical results with experimental results obtained in ref. [10]

Ra		$Nu_{0.25}$	$Nu_{0.75}$	$Nu_{1.1}$	$Nu_{1.25}$	$Nu_{1.75}$
10^6	Experimental Result	6.98	6.96	6.82	6.96	6.92
	Numerical Result	7.16	7.18	7.18	7.15	7.17
10^7	Experimental Result	no data	no data	no data	no data	no data
	Numerical Result	14.14	14.18	14.17	14.16	14.13
10^8	Experimental Result	26.60	26.58	26.52	26.58	26.60
	Numerical Result	27.31	27.50	28.10	27.70	27.20

refinement was carried out to demonstrate that the numerical results are not significantly dependent on the chosen numerical parameters. The following convergence criterion was adopted:

$$\left|\left(\frac{\partial U}{\partial X}+\frac{\partial V}{\partial Y}\right)_{i,j}\right|_{\max} < \varepsilon_1$$

$$\left|\frac{\Phi_{i,j}^{k+1}-\Phi_{i,j}^{k}}{\Phi_{i,j}^{k+1}}\right|_{\max} < \varepsilon_2 \qquad (7)$$

where ε_1 and ε_2 are 10^{-6} and 10^{-4} respectively, Φ indicates the physical variable of interest, and superscript k denotes the iteration index.

CODE VALIDATION

To validate the code and demonstrate the accuracy of numerical procedure used in the present work, the numerical results for $Pr = 7.0$ and $Ra = 10^6$ to 10^8 are compared with the experimental results in ref. [10]. Table 1 compares the average Nusselt numbers at five different positions $X = 0.25$, 0.75, 1.1, 1.25 and 1.75 respectively; and Figs. 2 and 3 compare the velocity and temperature profiles with the experimental results. These results are in good agreement with the experimental results demonstrating the reliability of the adopted numerical procedure. The average Nusselt numbers are slightly higher than those obtained

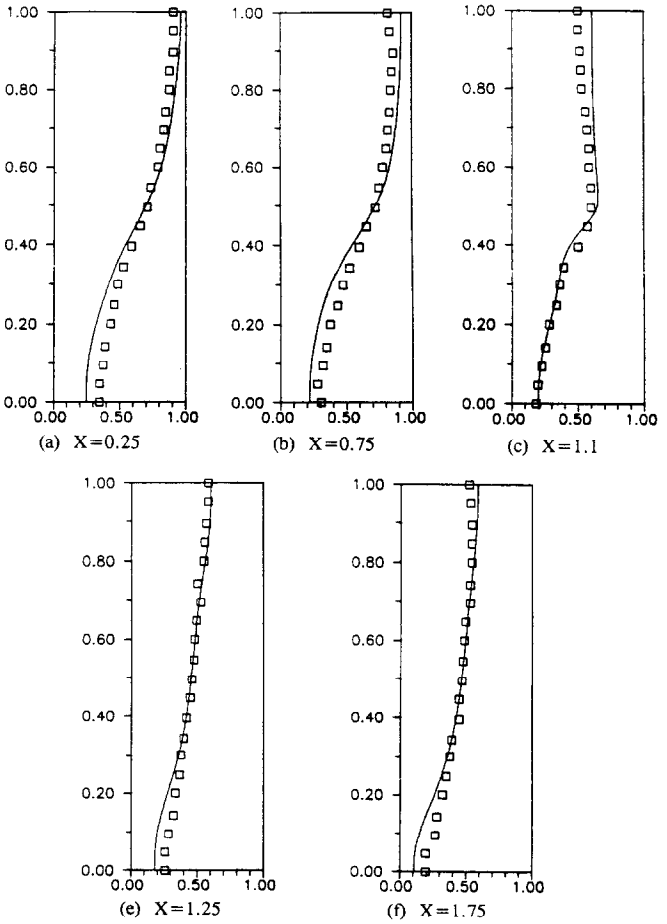

FIG. 3. Comparison of numerical and experimental results; temperature profiles at $X = 0.25$, 0.75, 1.1, 1.25, 1.75, $Ra = 10^6$.

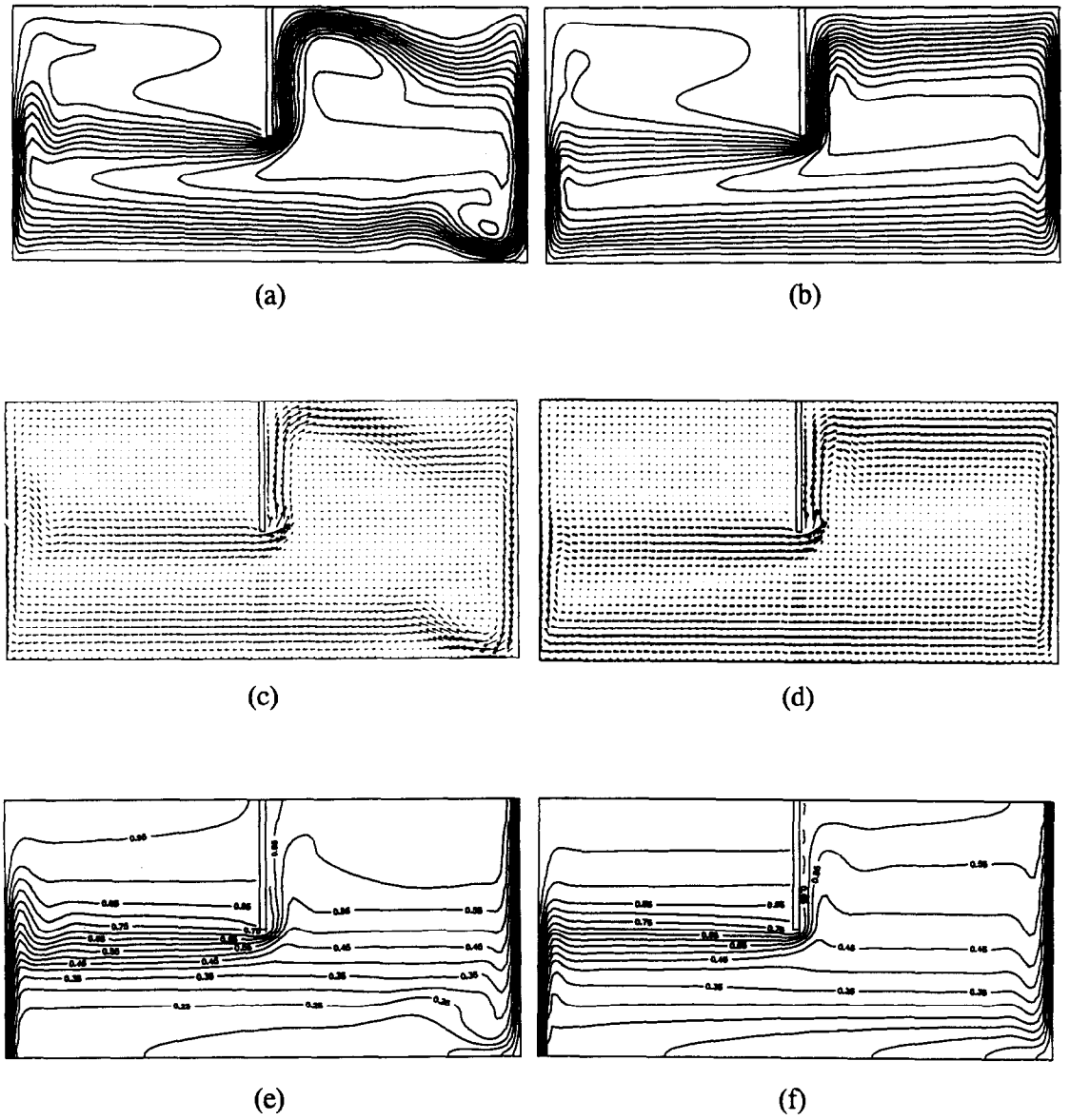

FIG. 4. Streamlines, vector fields and isotherms for $A_o = 0$. (a), (c), and (e) $Pr = 0.71$, $Ra = 10^7$; (b), (d), and (f) $Pr = 7.00$, $Ra = 10^7$.

experimentally [10]. The velocity and temperature distribution at these different positions are in excellent agreement with the corresponding experimental results.

RESULTS AND DISCUSSION

In the present investigation, the Rayleigh number is varied from 10^6 to 10^8. The Prandtl numbers used are 0.71 and 7.0, which correspond to air and water respectively. The details of the fluid flow and the temperature fields are presented below, with emphasis on comparison of natural convection results of air and water.

Fluid flow phenomenon

Fluid flow configurations of air and water in the form of streamlines are presented in Figs. 4–7 for Rayleigh numbers 10^6–10^8 and Prandtl numbers 0.71 and 7.0. Figure 4 presents the stream lines, velocity vectors, and isotherms for the cases of no opening in the partition plate. Here for water we observe a similar flow pattern as was observed by Nansteel and Greif [9]. In general, the flow is composed of three regions: a region of peripheral boundary-type flow, a relatively inactive core region, and a very weak or virtually no recirculation zone in the upper left-hand quadrant of the enclosure. The non-existence of recirculation is consistent with the findings of ref. [9], where it was noted that adiabatic partition yielded no recirculation.

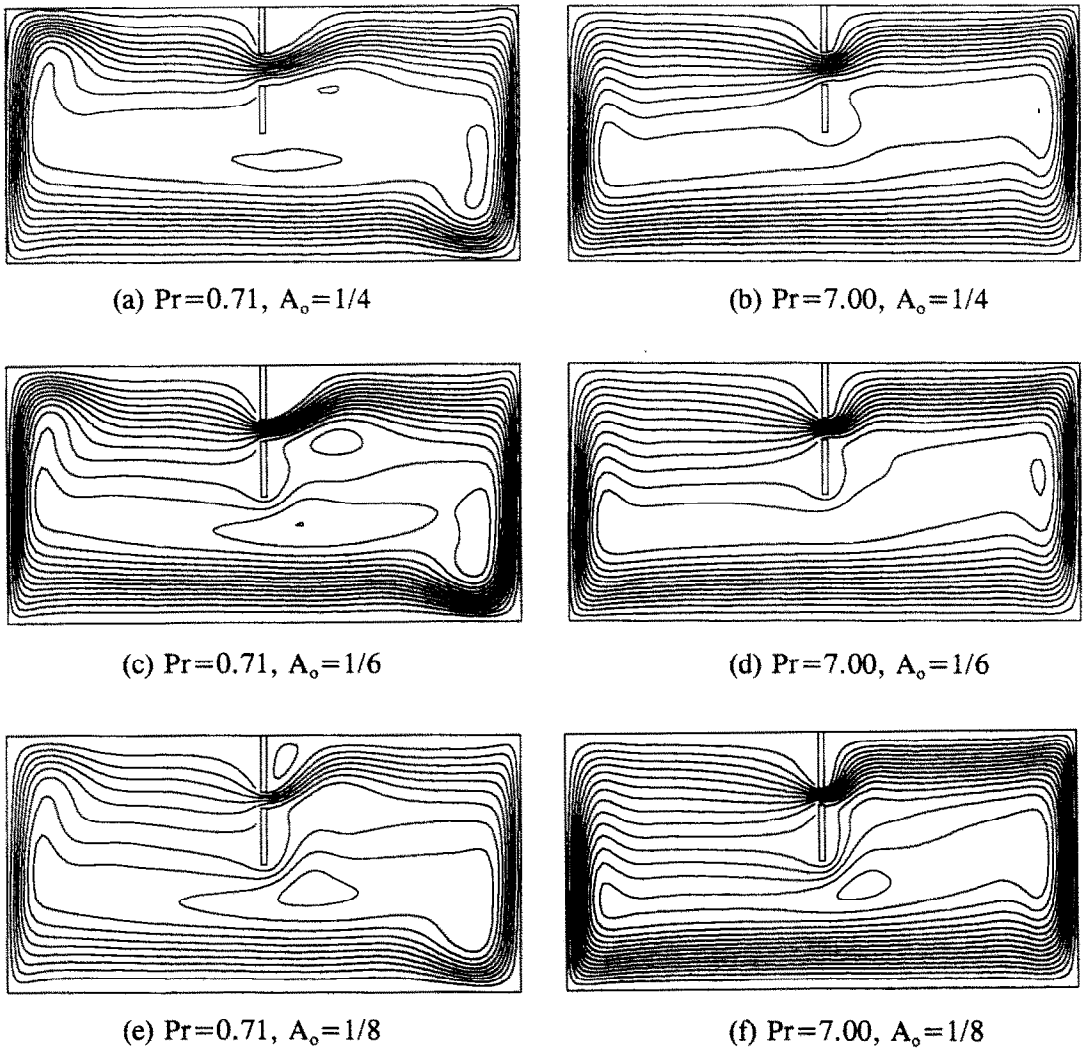

FIG. 5. Streamlines for water and air at $Ra = 10^6$. (a) $Pr = 0.71$, $A_o = 1/4$; (b) $Pr = 7.0$, $A_o = 1/4$; (c) $Pr = 0.71$, $A_o = 1/6$; (d) $Pr = 7.0$, $A_o = 1/6$; (e) $Pr = 0.71$, $A_o = 1/8$; (f) $Pr = 7.0$, $A_o = 1/8$.

The only difference noted between air and water with no opening in the partition is that for air we observed recirculation cells at the lower right hand corner and upper left hand corner on the cold side of the partition; and, for water such recirculation does not exist.

For the partition with an opening, we observe significantly different fluid flow phenomenon; even though the flow still has the characteristics of a boundary-type flow. The upward-moving flow along the hot wall divides into three streams, as described in ref. [10]. They are (1) a weak lower stream, (2) a middle main stream, and (3) an upper stream. The three streams tend to merge on the cold side of the partition. For water, the lower stream separates from the hot wall at a height of $Y \cong 1/2$, moves almost horizontally and turns around the bottom of the partition. For air, the fluid separates from the hot wall at a higher altitude than that for water. The flow characteristics are strongly dictated by the Rayleigh numbers and the partition opening ratios. For smaller opening ratios (A_o) and lower Rayleigh numbers, the lower stream is much stronger as shown in Fig. 5. At higher Rayleigh numbers this stream is very weak. This point can also be reflected by analyzing the velocity profiles at the plane of partition. Figure 8 compares non-dimensional horizontal velocities for water and air at the plane of the partition. From the figure it is obvious that the horizontal velocity near the bottom of the partition is much smaller at higher Rayleigh numbers compared to those at lower Rayleigh numbers. The middle main stream separates from the hot wall at an elevation corresponding to the location of the opening and flows horizontally through the opening. This main stream is the most dominant stream in determining the exchange flow rates between the two sides of the partition plate, this dominance is particularly

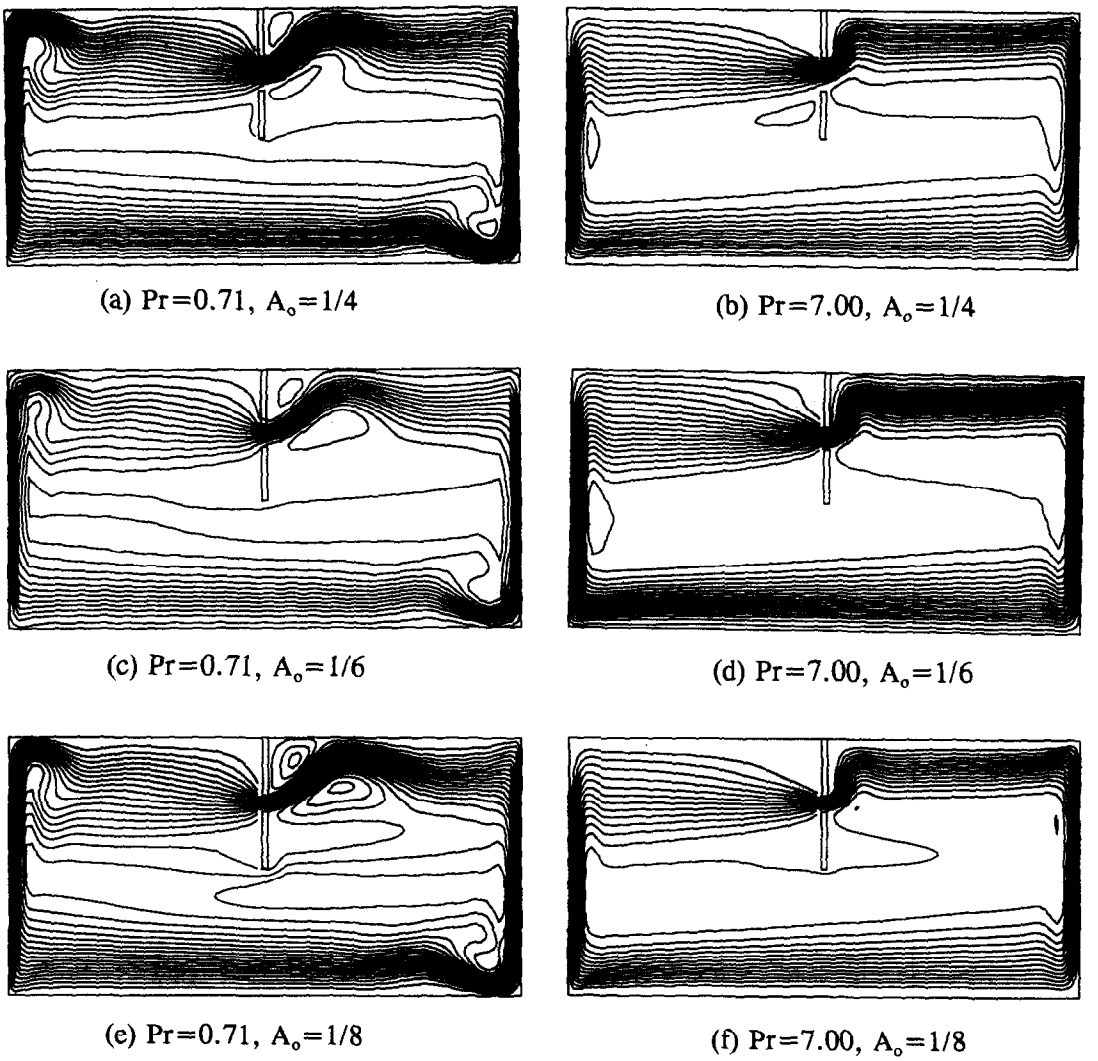

FIG. 6. Streamlines for water and air at $Ra = 10^7$. (a) $Pr = 0.71$, $A_o = 1/4$; (b) $Pr = 7.0$, $A_o = 1/4$; (c) $Pr = 0.71$, $A_o = 1/6$; (d) $Pr = 7.0$, $A_o = 1/6$; (e) $Pr = 0.71$, $A_o = 1/8$; (f) $Pr = 7.0$, $A_o = 1/8$.

large at high Rayleigh numbers (Fig. 7) where the top and bottom streams are very weak. The upper stream flows along the hot wall, turns along the top wall, and moves downward at the partition plate and eventually flows out through the opening. The three streams that merge on the cold side of the partition have different characteristics for water and air at the same Rayleigh numbers and opening ratios. For $Pr = 7.0$, i.e. for water, the merged stream attaches and flows along the cool side of partition, with no re-circulation, then turns and flows along the top wall. At $Pr = 0.71$, i.e. for air, the merged stream leaves the opening at an angle and then attaches to the top wall without ever attaching to the partition plate. This flow characteristic is more obvious at higher Rayleigh number and lower opening ratios as shown in Figs. 6(e) and (f) for Rayleigh number 10^7 and $A_o = 1/8$; or in Figs. 7(e) and (f) for Rayleigh number 10^8 and $A_o = 1/8$.

For air at higher Rayleigh numbers and smaller opening ratios, for example at $A_o = 1/8$, $Ra = 10^7$ in Fig. 6(e) and at $A_o = 1/8$, $Ra = 10^8$ in Fig. 7(e), separation of fluid occurs away from the merged stream and fluid recirculation is observed on the cool side of the partition. There is also a significant difference in the growth and thickness of the boundary layers for water and air. As expected with the increase in Rayleigh number, the boundary layer thickness at the two vertical walls decreases, for both water and air. But, as the fluid flows from the cold wall to the hot wall along the bottom of the enclosure, the thickness of the boundary layer decreases for water ($Pr = 7.0$) and increases for air ($Pr = 0.71$). This difference in the boundary layer growth is due to the presence of recirculation of air in the lower right corner of the cold chamber; for water such recirculation is not there. The growth in the boundary layer of air inhibits the

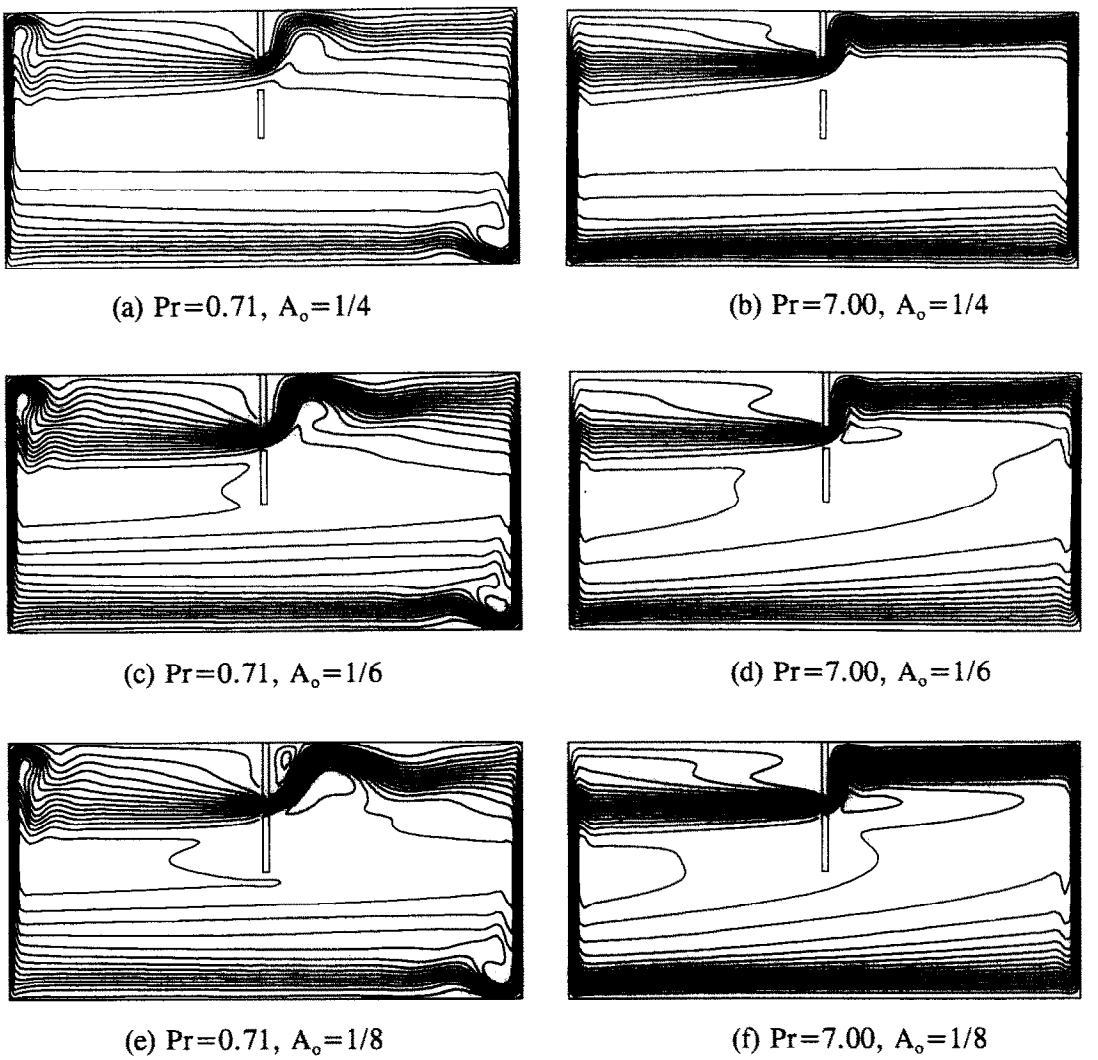

FIG. 7. Streamlines for water and air at $Ra = 10^8$. (a) $Pr = 0.71$, $A_o = 1/4$; (b) $Pr = 7.0$, $A_o = 1/4$; (c) $Pr = 0.71$, $A_o = 1/6$; (d) $Pr = 7.0$, $A_o = 1/6$; (e) $Pr = 0.71$, $A_o = 1/8$; (f) $Pr = 7.0$, $A_o = 1/8$.

exchange flow rate of the fluid between the chambers, and this may account for greater volume exchange flow rate for water as compared to air for the same Rayleigh number. Another difference in fluid flow pattern for air and water is the maximum horizontal velocity which occurs at the center of the opening. As shown in Fig. 8, the maximum velocity for water is larger than that for air. Both opening ratio and Rayleigh numbers have a significant effect on the maximum horizontal velocity at the plane of the opening. The maximum velocity becomes smaller when the opening ratio becomes larger. However, the opening ratio has very little effect on velocity distribution between the bottom of partition and bottom wall. It is apparent from the comparison of fluid flow configurations of air and water that the Prandtl number has a substantial effect on the flow configuration. It is noted that a small vortex on the upper right-hand corner of the partition which was reported in ref. [10], is not found in the present study. Only at $Pr = 0.71$ can this small vortex be seen.

Figure 9 presents isotherms for the cases investigated in this study at $Ra = 10^8$. For both water and air we observe thermal stratification of the fluid. This stratification is found to be stronger at higher Rayleigh numbers.

Heat transfer and exchange flow rate

Figure 10 presents the results of average Nusselt number and exchange flow rate defined by equation (6). Results show that an opened partition would increase the average Nusselt number by $13 \sim 24\%$ for both water and air, depending on the Rayleigh number and opening ratio. This increase in Nusselt number can be explained in the following way. From the velocity distribution at the partition plane as

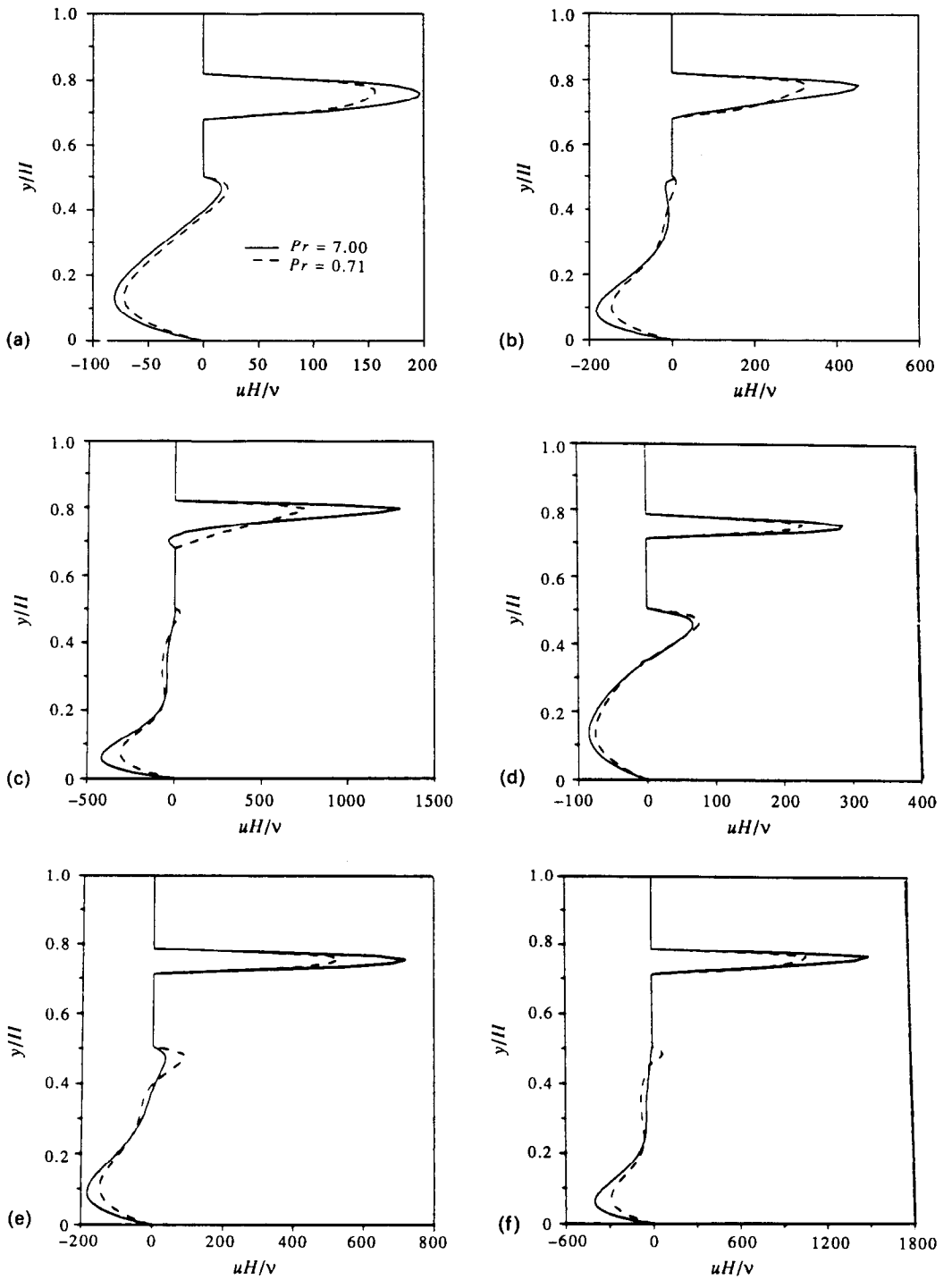

FIG. 8. Comparison of velocity profiles at opening position for both air and water. (a) $Ra = 10^6$, $A_o = 1/4$; (b) $Ra = 10^7$, $A_o = 1/4$; (c) $Ra = 10^8$, $A_o = 1/4$; (d) $Ra = 10^6$, $A_o = 1/8$; (e) $Ra = 10^7$, $A_o = 1/8$; (f) $Ra = 10^8$, $A_o = 1/8$.

shown in Fig. 8 and streamlines shown in Figs. 4–7 respectively, it can be seen that with an opened partition the hot fluid flows from the left half to the right half mainly through the opening. No hot fluid is trapped in the upper left-hand quadrant. But, with an unopened partition the boundary layer on the hot wall does not extend over the entire surface because most of the fluid separates from the hot wall at approximately $Y = 1/2$ and some hot fluid is trapped at the upper left-hand quadrant. This is disadvantageous to heat transfer. The opening ratio has a negligible effect on average Nusselt number, especially at high Ray-

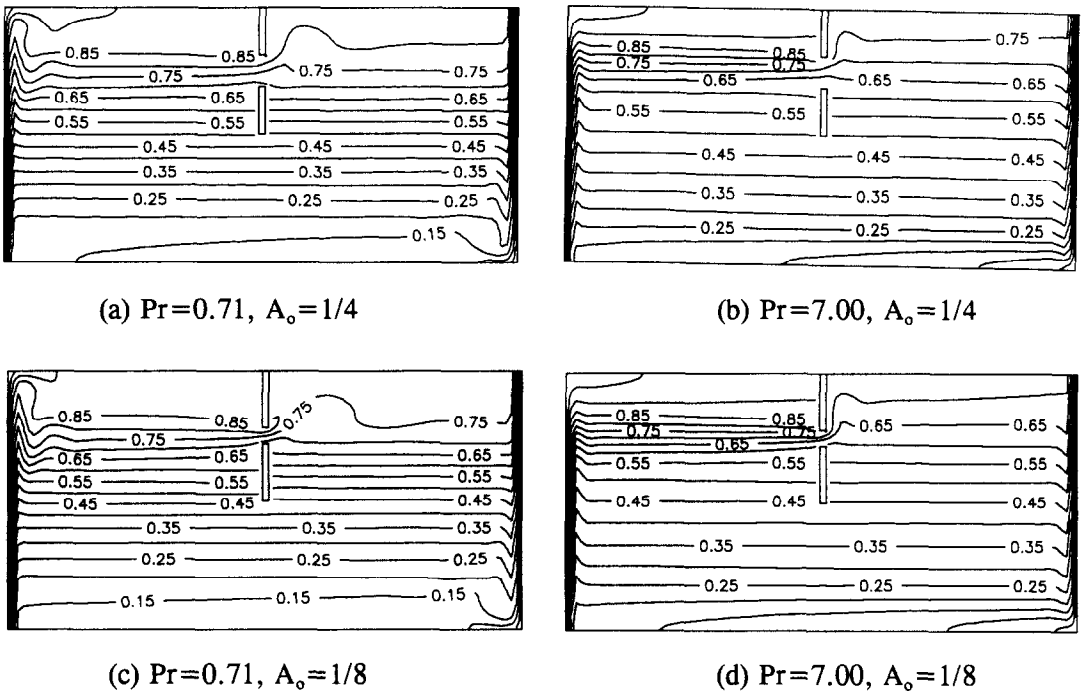

FIG. 9. Isotherms for water and air at $Ra = 10^8$. (a) $Pr = 0.71$, $A_o = 1/4$; (b) $Pr = 7.0$, $A_o = 1/4$; (c) $Pr = 0.71$, $A_o = 1/8$; (d) $Pr = 7.0$, $A_o = 1/8$.

leigh numbers. Depending on both the opening ratio and Rayleigh number, the average Nusselt numbers for water are about 2 ~ 5% larger than those for air.

Exchange flow rates, based on the fluid exchange rates at the partition plane, has practical significance in the investigation of indoor air quality. The measure of exchange flow rate is an indicator of contaminant exchange between rooms in the events of fire accidents. It is interesting to observe that, unlike the average Nusselt number, the opened partition reduces the exchange flow rates. For water the exchange flow rate is reduced by 5.68 ~ 15.2% and for air the reduction is 1 ~ 11.4%. The decrease in the exchange flow rate due to the presence of an opening in the partition can be explained by studying the streamlines (Figs. 5–7). It is noted that with the presence of the opening in the partition plate, most of the hot fluid from the hot wall side flows through the opening; and the mass between the two sides is conserved with a counter flow toward the bottom of the partition. Thus, the exchange flow rate is essentially determined by the flow rates through the opening, where the opening in the partition plate acts as a constriction which decreases the exchange flow rates. It is also observed that the exchange flow rate for water is 12 ~ 20% larger than that for air, indicating the effect of Prandtl number on the exchange flow rates. It can be noted that, there is a very little effect of the opening ratio on the exchange flow rates. With the decrease in opening ratios it is found that the volume exchange rate increases very slightly for both water and air (Fig. 10). Study of Fig. 8 reveals that as the opening ratio decreases the nondimensional horizontal velocity through the opening increases, but since the opening area is less at lower opening ratios, the net result is only a negligible increase in the average exchange flow rates at lower opening ratios.

CONCLUSIONS

This work presents a numerical solution for natural convection in a partitioned rectangular enclosure. Numerical computations are made using both air and water as the working fluids. Particular emphasis is placed on numerical solution at high Rayleigh number (up to 10^8) and on the comparison of the effect of different Prandtl number on fluid flow and heat transfer characteristics. The following conclusions are based on our findings.

(1) Flow configurations for air and water are different. Prandtl number has an important effect on the flow configuration.

(2) For the same Rayleigh number, geometry and boundary conditions, the average Nusselt number for water is about 2 ~ 5% larger than that of air.

(3) Compared with the unopened partition, an opened partition increases average Nusselt number by 13 ~ 24% for both air and water. This increase is larger at higher Rayleigh numbers. The effect of opening ratio on average Nusselt number is not very significant.

(4) Unlike the average Nusselt number, opened

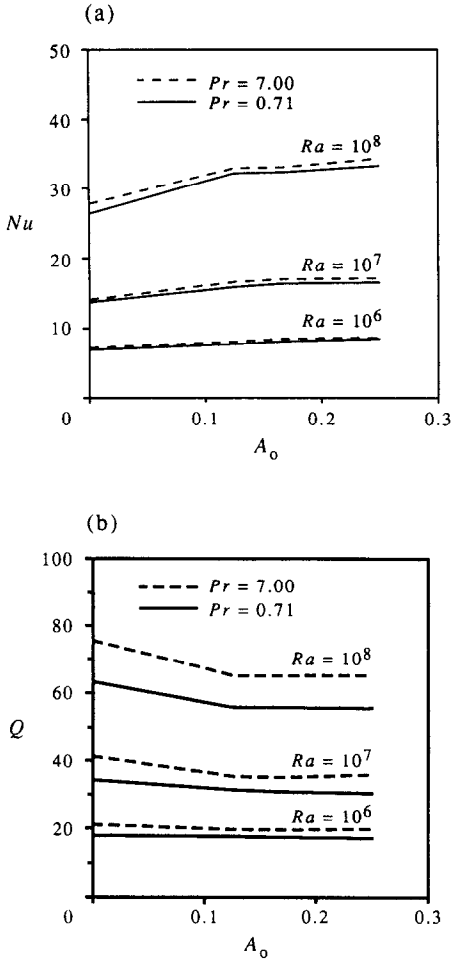

FIG. 10. Nusselt number (Nu) and exchange flow rate (Q).

partition reduces the exchange flow rate through the partition plane by 5.68 ~ 15.3% for water and by 1 ~ 11.4% for air. The opening ratio has a very small effect on the exchange flow rate. At the same Rayleigh number and geometry and boundary condition the exchange flow rate for water is 12 ~ 20% larger than that for air.

(5) Traditionally used water models to predict the natural convection of air give reasonable heat transfer results. The fluid flow characteristics for air are different from those of water. The maximum velocity and exchange flow rates reflect this point.

REFERENCES

1. W. G. Brown and K. R. Solvason, Natural convection heat transfer through rectangular openings in partitions—1, *Int. J. Heat Mass Transfer* **5,** 859–868 (1962).
2. W. G. Brown, Natural convection through rectangular openings in partitions—2, *Int. J. Heat Mass Transfer* **5,** 869–878 (1962).
3. M. Epstein, Buoyancy-driven exchange flow through small openings in horizontal partitions, *ASME J. Heat Transfer* **110,** 885–893 (1988).
4. M. Epstein and M. A. Kenton, Combined natural convection and forced flow through small openings in a horizontal partition, with special reference to flows in multicompartment enclosures, *ASME J. Heat Transfer* **111,** 980–987 (1989).
5. A. Bejan and A. N. Rossie, Natural convection in horizontal duct connecting two fluid reservoirs, *ASME J. Heat Transfer* **103,** 108–113 (1981).
6. N. Lin and A. Bejan, Natural convection in a partially divided enclosure, *Int. J. Heat Mass Transfer* **26,** 1867–1868 (1983).
7. J. Neymark, C. R. Boardman and A. Kirkpatrick, High Rayleigh number natural convection in partially divided air and water filled enclosure, *Int. J. Heat Mass Transfer* **32,** 1671–1679 (1989).
8. M. W. Nansteel and R. Greif, An investigation of natural convection in enclosures with two and three-dimensional partitions, *Int. J. Heat Mass Transfer* **27,** 561–571 (1984).
9. M. W. Nansteel and R. Greif, Natural convection in undivided and partially divided rectangular enclosures, *ASME J. Heat Transfer* **103,** 623–629 (1981).
10. K. S. Chen, A. C. Ku and C. H. Chou, Investigation of natural convection in partially divided rectangular enclosures both with and without an opening in the partition plate: Measurement results, *ASME J. Heat Transfer* **112,** 648–652 (1990).
11. K. S. Chen and P. W. Ko, Natural convection in a partially divided rectangular enclosure with an opening in the partition plate and isoflux side walls, *Int. J. Heat Mass Transfer* **34,** 237–246 (1991).
12. L. C. Chang, J. R. Lloyd and K. T. Yang, A finite difference study of natural convection in complex enclosure, *Proc. 7th Int. Heat Transfer Conf.*, Munich, pp. 183–188 (1982).
13. E. Zimmerman and S. Acharya, Free convection heat transfer in a partially divided vertical enclosure with conducting end walls, *Int. J. Heat Mass Transfer* **30,** 319–331 (1987).
14. S. Acharya and R. Jetli, Heat transfer due to buoyancy in a partially divided square box, *Int. J. Heat Mass Transfer* **33,** 931–942 (1990).
15. H. J. Shaw, C. K. Chen and J. W. Cleaver, Cubic spline numerical solution for two dimensional natural convection in a partially divided enclosure, *Numerical Heat Transfer* **12,** 439–455 (1987).
16. W. S. Fu, J. C. Perng and W. J. Shieh, Transient laminar natural convection in an enclosure partitioned by an adiabatic baffle, *Numerical Heat Transfer A* **16,** 325–350 (1989).
17. S. Lee and G. S. Dulikravich, Accelerated computation of viscous incompressible flows with heat transfer, *Numerical Heat Transfer B* **19,** 223–241 (1991).
18. S. V. Patankar, *Numerical Heat Transfer and Fluid Flow*. McGraw-Hill, New York (1980).
19. S. V. Patankar, A numerical method for conduction in composite materials, flow in irregular geometries and conjugate heat transfer, *Proc. Sixth Int. Heat Transfer Conf.*, Toronto, Vol. 3, pp. 297–302 (1978).
20. A. W. Date, Numerical prediction of natural convection heat transfer in horizontal annulus, *Int. J. Heat and Mass Transfer* **29,** 1457–1464 (1986).